

Low temperature heat capacity of amorphous systems: physics at nano-scales

Pragya Shukla

Department of Physics, Indian Institute of Technology, Kharagpur-721302, India

(Dated: April 2, 2022)

Abstract

We analyze the density of states and specific heat contribution of dispersion forces in an amorphous solid of nano-scales. Our analysis indicates a universal semi-circle form of the average density of states in the bulk of the spectrum along with a super-exponentially increasing behavior in its edge. The latter in turn leads to a specific heat, behaving linearly below $T < 1^\circ \text{K}$ even at nano-scales and agreeing with the experiments although the latter are carried out at macroscopic scales. The omnipresence of dispersion forces as microscopic scales indicates the application of our results to other disordered materials too.

I. INTRODUCTION

At low temperatures, structurally and orientationally disordered solids such as dielectric and metallic glasses, amorphous polymers and even crystals are experimentally observed to exhibit many universalities [1–3]. The theoretical understanding of this behavior is usually based on tunnelling two level systems (TTLS) intrinsic to disordered state [4, 5]. The existence of TTLS entities however in such a wide range of materials itself is not well-established (e.g. see [6–18]) and it is imperative to seek alternative theoretical explanations. In past, there have been many attempts in this context e.g. [19–25] but almost none of these studies analyze the issue at microscopic scales [7]. The primary focus of the present work is to bridge this information gap by the specific heat analysis at low temperature.

The appearance of universal features in a wide range of disordered systems strongly suggest the behavior to originate in fundamental type of interactions. This intuitively motivates us to consider the inter-molecular interactions, more specifically dispersion type VanderWaal forces among the molecules of the amorphous solid as the root cause for the behavior. The intuition comes from the omnipresence of these forces in all condensed phases thus making them promising candidates to decipher the experimentally observed universality.

Amorphous solids possess a rich and varied array of short to medium range topological order which originates from their chemical bonding and related interactions. The bonding interactions at short range (upto 1st and 2nd nearest neighbor molecular distances), are dictated by the valance force fields (covalent or ionic, also acting as mechanical constraints) but the medium range order (typically of the order of $10 - 30$ AA), is governed by the Vanderwaal interactions [26, 27]. Intuitively these varying structures at different length scales are expected to result in materials with very different physical properties. Any theory of experimentally observed universality therefore must take into account the microscopic structure of the solid and explain the emergence of system-independence of the physical properties at large scales; this is because the related experiments are usually carried out on macroscopic sizes. This also incites a natural query whether the universalities also appear at smaller length scales and if not then when and how much they deviate. The point to ponder is whether the observed universalities are emergent phenomenon due

to interactions at larger scale or even the molecular interactions within the short length scales (of medium range order) can give rise to them on their own. The query arises because the nano-materials exhibit physical and chemical properties that are significantly different from the corresponding properties of bulk materials [28–32]. It is therefore relevant to seek, identify and analyze the behavior of the sub-units (nano-scale structures, later referred as basic blocks) of the macroscopic glass solid.

Our primary focus in the present work is to understand the low temperature behavior of the specific heat for a basic block. Based on standard partition function approach, this requires a prior knowledge of the density of states and therefore its Hamiltonian \mathcal{H} . The latter, although acting in an infinite dimensional Hilbert space, can be represented by a large but finite-size matrix in a physically motivated basis, with the size dictated by energy-range of interactions. Due to complexity of the many-body interactions within the block, however, the matrix elements can not be exactly determined and can at best be described by their distribution over an ensemble of the replicas of H -matrix. Intuitively, the form of the distribution or the distribution parameters are expected to be system specific. The experimentally observed universality at low temperatures however suggests that the theoretical formulation should not depend on any system-specific details. We therefore will not assume any specific form of the distribution of the elements of H -matrix except that the latter must satisfy basic symmetry and conservation laws of the Hamiltonian.

The paper is organized as follows. Section II describes the Hamiltonian of a basic block as a collection of molecules and calculates the variance of its matrix elements in a physically motivated basis. The latter information is used in section III to derive the ensemble averaged density of states of the Hamiltonian which turns out to be a semi-circle in the bulk of the spectrum but growing super-exponentially in its edge (the later relevant for low temperature behavior). As the density is derived without using any system-specific information about the intra-molecular forces, it is applicable for a wide range of glasses including the network as well as the metallic ones. Section IV derives the specific heat of the basic block for the temperature ranges below and above Debye temperature and confirms its linear temperature dependence even at nanoscale sizes. We conclude in section V with a summary of our main ideas and results.

II. BASIC BLOCK HAMILTONIAN

Consider a nano-scale block of an arbitrary isotropic amorphous material, composed of g_0 molecules labeled as " k " with positions \mathbf{r}_k and masses m . The Hamiltonian of the block can be written as

$$\mathcal{H} = \mathcal{H}_0 + \mathcal{U}(\mathbf{r}_1, \mathbf{r}_2, \dots, \mathbf{r}_{g_0}) \quad (1)$$

where \mathcal{H}_0 is the total Hamiltonian of g_0 uncoupled (or free) molecules

$$\mathcal{H}_0 = \sum_{n=1}^{g_0} h_n(\mathbf{r}_n) \quad (2)$$

with $h_n(\mathbf{r}_n)$ as the Hamiltonian of the n^{th} molecule at position \mathbf{r}_n , consisting of intra-molecular interactions and \mathcal{U} as the sum over inter-molecular many-body interactions of g_0 molecules. The inter-molecular interactions being relatively weaker as compared to intra-molecular ones, \mathcal{U} can be considered as a perturbation on \mathcal{H}_0 and expanded as a series consisting of n -body contributions [33, 34]

$$\mathcal{U}(\mathbf{r}_1, \dots, \mathbf{r}_{g_0}) = \mathcal{U}^{es}(\mathbf{r}_1, \dots, \mathbf{r}_{g_0}) + \sum_{n=2}^{g_0} \sum_{q_1, q_2, \dots, q_n} \mathcal{U}^{(q_1, q_2, \dots, q_n)}(\mathbf{r}_{q_1}, \dots, \mathbf{r}_{q_n}) \quad (3)$$

where \mathcal{U}_{es} corresponds to 1st order perturbation correction consisting only of the electrostatic contribution and $\mathcal{U}^{(q_1, q_2, \dots, q_n)}$ as n -body polarization interactions (i.e including both dispersion as well as induction) among n molecules, labeled as " q_1 ", " q_2 " ..., " q_n ". The symbol $\sum_{q_1, q_2, \dots, q_n}$ corresponds to a summation over all possible n -body polarization interactions among all g_0 molecules.

A. Matrix Representation

For matrix representation of \mathcal{H} , we consider the eigen-basis of the non-interacting molecules, consisting of the direct-product of g_0 normalized single-molecule states in which the molecules are assigned to definite single-molecule states; (hereafter the basis will be referred as NIM). In general a single molecule can exist in infinitely many states of electronic, vibrational and rotational type; this would imply an infinite dimensional basis-space. To study the thermal effects at very low temperatures ($T < 30K$), it is however sufficient to consider only roto-vibrational levels in the electronic ground state of each isolated molecule

[35]. Assuming only \mathcal{N} such states of each molecule participate in the interaction, this gives the size of NIM basis space as

$$N = \mathcal{N}^{g_0}. \quad (4)$$

Let $|\mathcal{K}_n\rangle$ and $E_{\mathcal{K}_n}$, with $\mathcal{K}_n = 1, 2, \dots, \mathcal{N}$, be the eigenvectors and eigenvalues of a molecule, say "n": $\mathcal{H}_0^{(n)} |\mathcal{K}_n\rangle = E_{\mathcal{K}_n} |\mathcal{K}_n\rangle$. A typical basis-state in the $N \times N$ dimensional NIM basis can then be given as $|\mathcal{K}\rangle = \prod_{n=1}^g |\mathcal{K}_n\rangle$ with $|\mathcal{K}_n\rangle$ referring to the specific eigenvector of the n^{th} molecule which occurs in the product state $|\mathcal{K}\rangle$. (Note as the exchange interactions are neglected, the basis need not be anti-symmetrized). From eq.(2), \mathcal{H}_0 is a diagonal matrix in the NIM basis

$$\mathcal{H}_{0;\mathcal{KL}} \equiv \langle \mathcal{K} | \mathcal{H}_0 | \mathcal{L} \rangle = \sum_{n=1}^{g_0} E_{\mathcal{K}_n} \delta_{\mathcal{KL}} \quad (5)$$

and eq.(3) leads to

$$\mathcal{U}_{\mathcal{KL}} = \delta_{\mathcal{KL}} \mathcal{U}_{\mathcal{KL}}^{es} + (1 - \delta_{\mathcal{KL}}) \left(\sum_{n=2}^{g_0} \sum_{q^1, q^2, \dots, q^n} \mathcal{U}_{\mathcal{KL}}^{(q^1, q^2, \dots, q^n)} \right) \quad (6)$$

(Note the induction and dispersion interaction, causing transition of molecules from one state to another, contribute only to off-diagonal matrix elements (see chapter 4 of [33]) which motivates the choice of basis). Although an exact calculation of these matrix elements is possible only for simple molecules, they can be approximated by some well-established methods e.g. using model potentials or by a multi-pole expansion of the n -body operator; the coefficients of expansions are then determined by abinitio approaches [33].

The matrix elements given by eq.(6) are valid for both polar as well non-polar molecules. But to gain better insight without loss of generality, henceforth we focus on non-polar molecules. The 2nd term in eq.(6) then consists of dispersion interaction only. Contrary to induction, a n -body dispersion interaction results in change of the states of all n -molecules and therefore its contribution to a matrix element in the NIM basis is non-zero only if the pair of basis-states form an n -plet. (The latter refers to a pair of basis states $|\mathcal{K}\rangle, |\mathcal{L}\rangle$ which differ in eigenfunction contributions from n -molecules i.e $\mathcal{K}_m \neq \mathcal{L}_m$ with m taking n -values from the set $\{1, 2, \dots, g_0\}$). Eq.(6) can then be rewritten as

$$\mathcal{U}_{\mathcal{KL}} = \mathcal{U}_{\mathcal{KL}}^{(q^1, q^2, \dots, q^n)} \quad n - \text{plet}, \mathcal{K}_{q^1, q^2, \dots, q^n} \neq \mathcal{L}_{q^1, q^2, \dots, q^n} \quad (7)$$

For sufficiently large distance, say R between a molecule pair ($R > 10 a_0$ with $a_0 \approx 0.53$ AA as Bohr radius), the n -body term can be well-approximated by a multi-pole expansion in which the leading order term is of type R^{-3n} (arising from n -dipoles interaction) [33]. For qualitative estimates of the energy, it is sufficient to take the first term in the expansion and one can write

$$\mathcal{U}_{\mathcal{KL}}^{(q_1, q_2, \dots, q_n)} \approx \frac{C_{\mathcal{KL}}^{(3n)}}{|\mathbf{r}_{q_1} - \mathbf{r}_{q_2}|^3 \dots |\mathbf{r}_{q_n} - \mathbf{r}_{q_1}|^3}. \quad (8)$$

where $C_{\mathcal{KL}}^{(3n)}$ is the coefficient of term corresponding to n -dipoles interaction in multi-pole expansion of $\mathcal{U}_{\mathcal{KL}}$. Further $\mathcal{U}_{\mathcal{KK}}^{es}$, the expectation value of the electrostatic energy for the set of g_0 molecules in state \mathcal{K} , can also be represented by a multi-pole expansion; here the leading order term depends on the point symmetry group of the molecules (see section 2.B of [39]). As the static dipole moment of non-polar molecules is zero in the ground state, the leading term comes from the mono-pole-quadrupole moment and is proportional to R^{-3} . In case of neutral molecules, however, the contribution from these terms is zero and one has to consider the next significant term which is quadrupole-quadrupole interaction (R^{-5}) if the quadrupole moment of the molecule is non-zero. Thus assuming that the molecules have zero dipole moment even in the excited states (vibrational), the leading term is proportional to $1/R^5$. For a set of g_0 molecules, the additivity of electrostatic energy then gives $\mathcal{U}_{\mathcal{KK}}^{es}(\mathbf{r}_1, \dots, \mathbf{r}_{g_0}) \approx C_{\mathcal{KK}}^{es} \sum_{\substack{i,j=1; \\ i>j}}^{g_0} \frac{1}{|\mathbf{r}_i - \mathbf{r}_j|^5}$ where $C_{\mathcal{KK}}^{es}$ is the strength of electrostatic interaction (of quadrupole-quadrupole type) for the molecules in the state \mathcal{K} (i.e n^{th} molecule in state \mathcal{K}_n for $n = 1 \rightarrow g_0$). The mean values for the quadrupole moment for a range of molecules can be of the order of $1 - 5 \text{ amu}$ ($10^{-40} \text{ C} - m^2$) (see Table III of [39]) and the contribution from the quadrupole-quadrupole interaction for two isolated molecules at a typical molecular distance of ~ 5

AA is of the order of $10^{-19} J$. The interaction however depends on the orientation of the molecular-pair too and can be positive, negative as well as zero (see section 3.4.2 of [33]). The net electrostatic contribution from $g_0(g_0 - 1)/2$ pairs of a cluster of $g_0 \gg 1$ randomly oriented but homogeneously distributed molecules within a basic block is therefore expected to be negligible.

Based on the above, the matrix elements of \mathcal{H} can now be approximated as

$$\mathcal{H}_{\mathcal{KL}} \approx \sum_{n=1}^{g_0} E_{\mathcal{K}_n} \quad \text{for } \mathcal{K} = L \quad (9)$$

$$\approx \frac{C_{\mathcal{KL}}^{(3n)}}{|\mathbf{r}_{q1} - \mathbf{r}_{q2}|^3 \dots |\mathbf{r}_{qn} - \mathbf{r}_{q1}|^3} \quad \text{for } \mathcal{K} \neq L. \quad (10)$$

B. Statistics of the Matrix Elements

As discussed in [38] and also later in section IV, the standard formulation of the statistical properties of the amorphous block is based on a prior knowledge of its density of states. But, due to an instantaneous nature of the interaction, \mathcal{U} is subjected to system dependent fluctuations; this in turn leads to randomization of the matrix elements of $\mathcal{H}_{\mathcal{KL}}$. As a consequence, the behavior of the "Hamiltonian" \mathcal{H} is best described by an ensemble of \mathcal{H} -matrices, consisting of the independent ensembles of \mathcal{H}_0 and \mathcal{U} -matrices. With help of eqs.(5,6), the ensemble average of the matrix element $\mathcal{H}_{\mathcal{KL}} = \mathcal{H}_{0\mathcal{KL}} + \mathcal{U}_{\mathcal{KL}}$ can be written as

$$\langle \mathcal{H}_{\mathcal{KL}} \rangle = \sum_{n=1}^{g_0} \langle h_{n;\mathcal{K}\mathcal{K}} \rangle \delta_{\mathcal{KL}} + \langle \mathcal{U}_{\mathcal{KL}} \rangle = \sum_{n=1}^{g_0} \langle E_{\mathcal{K}_n} \rangle \delta_{\mathcal{KL}} + \langle \mathcal{U}_{\mathcal{KL}} \rangle \quad (11)$$

where $\langle \mathcal{U}_{\mathcal{KL}} \rangle$ is given by an ensemble average of eq.(7) (along with eq.(8)).

A typical many body contribution can be both attractive as well as repulsive type and depends on the mutual orientation of the molecules. Under conditions in which all mutual orientations of the molecules are equally probable, the average of $C_{\mathcal{KL}}^{(3n)}$ over an ensemble of molecules can safely be assumed to be zero. This implies $\langle \mathcal{U}_{\mathcal{KL}} \rangle \approx \frac{\langle C_{\mathcal{KL}}^{(3n)} \rangle}{|\mathbf{r}_{q1} - \mathbf{r}_{q2}|^3 \dots |\mathbf{r}_{qn} - \mathbf{r}_{q1}|^3} \approx 0$. Further as a single molecule energy state can take both positive as well as negative values over an ensemble, its average over an ensemble is zero too i.e $\langle E_{\mathcal{K}_n} \rangle = 0$. (It is worth mentioning here that statistical behavior of the single molecule states for many molecules can be well-described by standard random matrix ensembles e.g. Gaussian orthogonal ensemble or GOE in short [48]). Eq.(11) then gives $\langle \mathcal{H}_{\mathcal{KL}} \rangle \approx 0$. Further ignoring the the correlations between \mathcal{H}_0 and \mathcal{U} , the variance $v_{\mathcal{KL}} = \langle (\mathcal{H}_{\mathcal{KL}})^2 \rangle - \langle \mathcal{H}_{\mathcal{KL}} \rangle^2$ becomes

$$v_{\mathcal{K}\mathcal{K}} \approx \sum_{n=1}^{g_0} \langle E_{\mathcal{K}_n}^2 \rangle = g_0 \nu_0, \quad v_{\mathcal{KL}} \approx \frac{\langle (C_{\mathcal{KL}}^{(3n)})^2 \rangle}{|\mathbf{r}_{q1} - \mathbf{r}_{q2}|^6 \dots |\mathbf{r}_{qn} - \mathbf{r}_{q1}|^6}. \quad n - \text{plet}, \mathcal{K}_{q1,q2,\dots,qn} \neq \mathcal{L}_{q1,q2,\dots,qn}. \quad (12)$$

with $\nu_0 = \langle E_{\mathcal{K}_n}^2 \rangle$ as the variance (the square of the line-width) of the vibrational energy-levels of a single isolated molecule Hamiltonian $\mathcal{H}_0^{(n)}$; It must be noted that the natural

line-width of a typical vibrational level due to Heisenberg uncertainty is negligible at very low temperatures; taking the natural line width of a typical vibrational level $\sim 10^{-11} \text{ cm}^{-1}$ ($\approx 10^{-34} \text{ J}$) gives $\nu_0 \sim (10^{-34})^2 \text{ J}^2$. Taking $g_0 \sim 10$ (see [38]) gives $v_{\mathcal{K}\mathcal{K}} \sim 10^{-67} \text{ J}^2$. Similarly the correlation $\langle \mathcal{H}_{\mathcal{K}\mathcal{L}} \mathcal{H}_{mn} \rangle_e = 0$ if $(k, l) \neq (m, n)$; this is again due to presence of both positive as well as negative contributions which on summation cancel each other.

As the basis pair \mathcal{K}, L refer to the vibrational states of the electronic ground state, the coefficients $C_{\mathcal{K}L}^{(3n)}$ are expected to be of the same order for all such basis-pairs and can be approximated by their average value over all states. Let us define \mathcal{C}_{3n}^2 as the mean square of the coefficient of the n -dipole interaction, respectively, with averaging over all the states as well over the ensemble (equivalent to averaging over all orientations):

$$\mathcal{C}_{3n}^2 = \frac{1}{N^2} \sum_{\mathcal{K}, L} \langle (C_{\mathcal{K}L}^{(3n)})^2 \rangle. \quad (13)$$

Fortunately a determination of the density of the states of the basic block requires a knowledge only of $\sum_{\mathcal{L}} v_{\mathcal{K}L}$ i.e summing it over all N basis states for a fixed \mathcal{K} . Approximating the contributions from all single molecule vibrational states undergoing dipole transition as almost same, the sum can then be rewritten as

$$\sum_{\mathcal{L}=1}^N v_{\mathcal{K}L} \approx g_0 \nu_0 + \sum_{n=2}^{g_0} \eta^n \mathcal{C}_{3n}^2 \sum_{\substack{q_1, \dots, q_n=1 \\ q_1 \neq q_2 \dots \neq q_n}}^{g_0} \frac{1}{|\mathbf{r}_{q_1} - \mathbf{r}_{q_2}|^6 \dots |\mathbf{r}_{q_n} - \mathbf{r}_{q_1}|^6}. \quad (14)$$

with $\eta = \mathcal{N} - 1$ as the number of allowed dipole transitions among the \mathcal{N} eigenstates of a single molecule from a fixed state \mathcal{K}_q . Note here $(C_{\mathcal{K}L}^{(3n)})^2$ is first replaced by \mathcal{C}_{3n}^2 which then permits the replacement of the sum $\sum_{\mathcal{L}=1}^N$ by the equivalent sums $\sum_{n=2}^{g_0} \sum_{\substack{q_1, \dots, q_n=1 \\ q_1 \neq q_2 \dots \neq q_n}}^{g_0}$; the latter sum here corresponds to, for a given n , to all n -molecules which undergo transition from their respective single-particle states in \mathcal{K} to those in \mathcal{L} . Eq.(14) can further be simplified as follows: as n - body dipole-dipole interaction contains a factor of r^{3n} , four-body and higher many-body terms are expected to be less important. Besides, no more than four atoms can be in mutual contact (see page 14, section 10.2 of [33]). For order of magnitude calculations, therefore, it suffices to keep the contribution from the nearest neighbor molecules (referred by z) only; (note, as VW forces in amorphous systems are inter-cluster forces i.e between primary structures such as rings, chains or layers etc, the nearest neighbours considered above are those present on adjacent primary structures). Also note that the total number of states \mathcal{L} forming a n -plet (defined above eq.(7)) with a given state \mathcal{K} and involving

transitions of nearest neighbor molecules only is $z \mathcal{N}^n$. This leads to

$$\sum_{\mathcal{L}=1}^N v_{\mathcal{KL}} \approx g_0 \nu_0 + \frac{z_{C_1} g_0 \eta^2 C_6^2}{2 (2R_v)^{12}} + \frac{z_{C_2} g_0 \eta^3 C_9^2}{2 (2R_v)^{18}} \quad (15)$$

where $2R_v$ is the distance of closest approach between two nearest neighbor molecules interacting by dispersion interaction, z as the number of nearest neighbors of a given molecule and g_0 as the total number of molecules in the block. Detailed studies of the higher order dispersion coefficient C_{3n} for various molecules indicate their rapid decay with increasing n (e.g see Table 10.1 and section 10.2 of [33]). Taking the typical distances between neighboring molecules of the order of 5

AA , $C_6 \sim 10^{-78} J - m^6$ and $C_9 \sim 10^{-108} J - m^9$, it is easy to check that the contribution from the terms containing ν_0 and C_9 is negligible as compared to the term with C_6 [41, 42]. For \mathcal{KL} -pairs forming the lower plets e.g 2,3-plets, it is easy to check that $v_{\mathcal{KL}} \gg v_{\mathcal{KK}}$. Referring the sum in eq.(15) as $\frac{1}{2b^2}$ for later use, it can then be approximated as

$$\frac{1}{2b^2} = \sum_{\mathcal{L}=1}^N v_{\mathcal{KL}} \approx \frac{z g_0 \eta^2 C_6^2}{2 (2R_v)^{12}}. \quad (16)$$

As discussed in next section, b appears as a measure of the bulk-spectrum width and plays an important role in our analysis. C_6 can further be written in terms of the Hamaker constant A_H (a constant for materials) i.e $A_H \approx \pi^2 C_6 \rho_n^2$, with ρ_n as the number density of the molecules. Taking $\Omega_{\text{eff}} = \frac{1}{\rho_n}$ as the average volume available to a typical glass molecule, we have

$$\Omega_{\text{eff}} = s_m (R_v + R_m)^3 \approx (1 + y)^3 \Omega_m \quad (17)$$

with Ω_m the molar volume: $\Omega_m = s_m R_m^3$, with s_m as a structure constant e.g. $s_m = 4\pi/3$ assuming a spherical shape for the molecule. Here R_v is half the distance between two nearest neighbor molecules; the 2nd equality in eq.(17) follows by writing $R_v = y R_m$. The above in turn gives

$$C_6 \approx \frac{A_H (\Omega_{\text{eff}})^2}{\pi^2} \approx \frac{s_m^2}{\pi^2} (1 + y)^6 R_m^6 A_H \quad (18)$$

Further as discussed in [38],

$$g_0 = \frac{\Omega_b}{\Omega_{\text{eff}}} \approx \frac{1}{(1 + y)^3} \left(\frac{R_0}{R_m} \right)^3 = \frac{64 y^3}{(1 + y)^3} \quad (19)$$

Based on the stability analysis of amorphous systems structure, z is predicted to be of the order of 3 (for a three dimensional block). Further, the intermolecular interactions being rather weak, they can mix very few single molecule levels. The dipole nature of these interactions further suggest $\mathcal{N} = 3$ (the number of relevant vibrational energy levels in a molecule); this in turn implies $\eta = 2$. The above on substitution in eq.(16) leads to

$$b \approx \frac{36}{\eta \sqrt{z} g_0 A_H} \frac{y^6}{(1+y)^6} = \frac{9}{4 \sqrt{3} A_H} \left(\frac{y}{1+y} \right)^{9/2} \quad (20)$$

Experimental data of some standard glasses suggest that R_v is typically of the same order as R_m . Hereafter we use $y = \frac{R_v}{R_m} \sim 1$ in our quantitative analysis. Eq.(19) then gives $g_0 = 8$.

Determination of A_H : for materials in which spectral optical properties are not available, two refractive-index based approximation for A_H namely, standard Tabor-Winterton approximation (TWA) and single oscillator approximation (SOA), provide useful estimates [44]. As indicated by previous studies, TWA is more appropriate for low refractive index materials (for $n < 1.8$); A_H in this case is given as (see eq.(11.14) of [43, 44])

$$A_H \approx \frac{3\hbar\nu_e}{16\sqrt{2}} \frac{(n_0^2 - 1)^2}{(n_0^2 + 1)^{3/2}} \quad (21)$$

with n_0 as the refractive index at zero frequency and ν_e as the characteristic absorption frequency in the ultra-violet (also referred as the plasma frequency of the free electron gas, with a typical value is $\nu_e = 3 \times 10^{15}$ for most ceramics). Further n_0 and ν_e in eq.(21) can be obtained by the standard routes (e.g. Cauchy's Plots or other available formulas) [44]: $n^2(\nu) - 1 = \mathcal{G}_{uv} + \frac{\nu^2}{\nu_e^2} (n^2(\nu) - 1)$. For cases, where the frequency-dependence of n is known either as an exact formula (e.g. V52, BALNA, LAT) or available for two or more frequencies (see *appendix B*), we determine ν_e and $n_0 = \sqrt{1 + \mathcal{G}_{uv}}$ by least square fit to plot $(n^2 - 1)$ vs $(n^2 - 1)/\lambda^2$. (Note eq.(21) is applicable for the case for two molecules interacting by VW interaction with vacuum as the intervening medium, with zero frequency contribution neglected; see eq.(11.14) of [43, 44]).

For materials with higher indexes (for $n > 1.8$) however TWA is found to be increasingly poor; instead, the single oscillator approximation (SOA) [44] is closer to the exact values

$$A_H \approx 312 \times 10^{-21} \frac{(n^2 - 1)^{3/2}}{(n^2 + 1)^{3/2}} J \quad (22)$$

with n as the available value of refractive index; for our calculation, we choose $n = n_0$.

Table I displays n_0 values along with ν_e values for the 18 glasses; (although the latter is not used for the higher index cases but is included here for the sake of completeness). The corresponding A_H values obtained by either eq.(21) or eq.(22) are also given the table along with b values from eq.(20).

III. DENSITY OF STATES

At very low temperatures, the induced dipole interactions result in excitations among vibrational energy levels of molecules (not strong enough to excite the electronic states and the chemical bonding prevents the rotation of molecules). In this section, we derive the ensemble averaged density of the states which participate in these excitations.

We proceed as follows: the many body density of states $\rho(e) = \sum_n \delta(e - e_n)$ of the Hamiltonian \mathcal{H} (eq.(1)) can be expressed in terms of the standard Green's function formulation: $\rho(e) = -\frac{1}{\pi} \text{Im} G(z)$ with $G(z) = \text{Tr} \frac{1}{\mathcal{H} - z}$ and z as a complex number. The ensemble averaged density of states can then be written as [45]

$$\langle \rho(e) \rangle = -\frac{1}{\pi} \text{Im} \langle G(z) \rangle \quad (23)$$

One can further write $\langle G(z) \rangle$ in terms of the moments $T_n \equiv \langle \text{Tr} \mathcal{H}^n \rangle$:

$$\langle G(z) \rangle = \langle \text{Tr} \frac{1}{\mathcal{H} - z} \rangle = -\frac{1}{z} \sum_{n=0}^{\infty} \frac{1}{z^n} T_n \quad (24)$$

It is easy to calculate the first three moments. As discussed in section II, $\langle \mathcal{H}_{\mathcal{K}\mathcal{L}} \rangle = 0$, $\langle \mathcal{H}_{\mathcal{K}\mathcal{L}}^2 \rangle = v_{\mathcal{K}\mathcal{L}}$ and $\langle \mathcal{H}_{\mathcal{K}\mathcal{L}} \mathcal{H}_{\mathcal{M}\mathcal{N}} \rangle = 0$ if $(\mathcal{K}, \mathcal{L}) \neq (\mathcal{M}, \mathcal{N})$ with $v_{\mathcal{K}\mathcal{L}}$ given by eq.(12). This gives $T_0 = N$, $T_1 = 0$ and

$$T_2 = \sum_{\mathcal{K}, \mathcal{L}} v_{\mathcal{K}\mathcal{L}} = \frac{N}{2b^2} \quad (25)$$

where b is given by eq.(20). To obtain higher order traces, we expand $\text{Tr} \mathcal{H}^n$ in terms of the matrix elements,

$$\text{Tr} \mathcal{H}^n = \sum_{\mathcal{K}_1, \mathcal{K}_2, \dots, \mathcal{K}_n} \mathcal{H}_{\mathcal{K}_1 \mathcal{K}_2} \mathcal{H}_{\mathcal{K}_2 \mathcal{K}_3} \dots \mathcal{H}_{\mathcal{K}_{n-1} \mathcal{K}_n} \mathcal{H}_{\mathcal{K}_n \mathcal{K}_1} \quad (26)$$

As clear, the trace operation ensures that the terms always have a cyclic appearance. Further in evaluating T_n for $N \rightarrow \infty$, only pairwise (binary) correlations will be of consequence. This is because the sum containing the same matrix element repeatedly are of the lower order in

N than the sums with pairs. In the limit of large N , therefore only the latter terms have to be considered (see *appendix A*, also section 3.1.5 of [45]).

In large N -limit, T_{2n} can then be approximated as

$$T_{2n} \approx \frac{1}{n+1} \binom{2n}{n} \frac{N}{2^n b^{2n}} \quad (27)$$

Similarly, with $\langle \mathcal{H}_{KL} \rangle = 0$, all odd order moments vanish:

$$T_{2n+1} \rightarrow 0 \quad (28)$$

Substituting the above results in eq.(24), we get

$$\begin{aligned} \langle G(z) \rangle &\approx -\frac{N}{z} \sum_{n=0}^{\infty} \frac{1}{n+1} \binom{2n}{n} \left(\frac{1}{2 b^2 z^2} \right)^n \\ &= -N z b^2 \left[1 - \left(1 - \frac{2}{b^2 z^2} \right)^{1/2} \right] \end{aligned} \quad (29)$$

Now writing $z = e + i\epsilon$ and taking the imaginary part of the above then gives

$$\langle \rho_{bulk}(e) \rangle = \frac{Nb}{2\pi} \sqrt{2 - (be)^2}. \quad (30)$$

As clear from the above, the bulk of the spectrum, with its width as $2\sqrt{2}/b$ and mean level spacing $\Delta_b \approx \frac{\pi\sqrt{2}}{Nb}$, depends on the single parameter b given by eq.(20) which is later referred as the *bulk-spectrum parameter*. As b depends on the average properties of the many body inter-molecular interactions, it is not expected to vary much from one system to another. This is also indicated by eq.(20). For later use, we shift the origin of the spectrum to $e = -\sqrt{2}/b$ and redefine $b = b_0\sqrt{2}$ which gives

$$\langle \rho_{bulk}(e) \rangle = \frac{Nb_0}{\pi} \sqrt{b_0 e (2 - b_0 e)} \quad (31)$$

As displayed in table I for 18 non-metallic glasses, $b \sim 10^{17} - 10^{18} J^{-1}$.

Eq.(31) is analogous to the bulk level-density of a Gaussian orthogonal ensemble (GOE) although the derivation given above does not assume any specific distribution of the matrix elements of the Hamiltonian; (a GOE refers to an ensemble of real-symmetric matrices with independent Gaussian distributed matrix elements with zero mean and variance of the diagonal twice that of the off-diagonal). A same expression was also obtained in [46] for the

bulk level density of a sparse random matrix (with its non-zero elements randomly taking values $0, \pm 1$). Indeed the semi-circle behavior of the bulk level density is known to be valid for a wide range of the matrix elements distributions with finite moments, (typical of dense matrices, irrespective of the nature of their randomness) [47, 49]. As in our case, the number of non-zero off-diagonals ($\approx N \sum_{p=1}^{g_0} {}^{g_0}C_p \eta^p$) is much larger than the diagonals (total N of them), H *effectively* behaves as a dense matrix and a semi-circle behavior of the level density is expected. An alternative reasoning for GOE type density of states can also be given as follows: as both \mathcal{H}_0 and \mathcal{U} consist of the contributions from many independent random terms, the central limit theorem predicts the distribution of their matrix elements to be Gaussian type. With many non-zero off-diagonals, the ensemble of \mathcal{H} matrices behaves *effectively* as a GOE. Following the above reasoning, the ensemble averaged edge level density $\langle \rho_{edge}(e) \rangle$ for \mathcal{H} can be modeled by that of a GOE too. Using a generic form, one can write

$$\langle \rho_{edge-t}(e) \rangle = \frac{N b_0}{\sqrt{\lambda}} f_t(\lambda b_0 e). \quad (32)$$

with $f_t(x)$ in case of a GOE is (with $t = L, U$, short form for lower and upper edge, respectively)

$$f_L(x) \approx x Ai^2(-x) + (Ai'(-x))^2 + \frac{1}{2} Ai(-x) E(-x) \quad \text{at lower edge } -\infty < x \quad (33)$$

$$f_U(x) \approx -(x-2) Ai^2(x-2) + (Ai'(x-2))^2 + \frac{1}{2} Ai(x-2) E(x-2) \quad \text{at upper edge } 2 < x \quad (34)$$

with $E(x) \equiv \int_{-\infty}^x Ai(y) dy$, with $Ai(y)$ as the Airy function of the first kind. For later use, it is worth noting that Airy-function asymptotics of eqs.(33,34) leads to a super-exponential form for $f_L(x)$ for $x < 0$ (*appendix B*)

$$f_L(x) \sim \frac{1}{\sqrt{|x|}} e^{-\sqrt{|x|^3}}. \quad (35)$$

and a square-root form for $x > 0$,

$$f_L(x) \approx \frac{\sqrt{c_0^2 + x}}{\pi} + \frac{1}{\pi x} \cos\left(\frac{2}{3} x^{3/2}\right). \quad (36)$$

where $c_0 = 0.1865 \pi$. As expected $f(x)$ is non-zero at $x = 0$; (note $f(x) = 0$ would imply a gap at $x = 0$ instead of smooth connection with the bulk density). Substitution of eq.(36) in eq.(32) gives

$$\langle \rho_{edge-l}(e) \rangle \approx \frac{N b_0 \xi}{\pi} \sqrt{c_0^2 + \lambda b_0 e} \quad (e > 0) \quad (37)$$

Thus, for $e > 0$, the edge behavior smoothly connects with the beginning of bulk of the ensemble averaged level density (see eq.(31) and figure 1).

Contrary to bulk, the edge-density depends on two parameters b and λ ; the latter, governing the decay of density of states in the lower edge, can be referred as the *edge-spectrum parameter*. Here λ is dimensionless and satisfy the requirement that $\langle \rho_{edge}(e) \rangle = \langle \rho_{bulk}(e) \rangle$ near $e \sim e_0$. For the GOE case, we have

$$\lambda = \lambda_0 N^{2/3} = \mathcal{N}^{2g_0/3} \lambda_0 = 3^{16/3} \lambda_0 \quad (38)$$

with λ_0 is a constant: $\lambda_0 \approx \sqrt{2}$. The 2nd equality in the above follows from $\mathcal{N} = 3$ and $g_0 \approx 8$ (see text below eq.(19). For later use, it is necessary to determine the point, say e_0 , where the edge of the spectrum meets the bulk; as discussed in *appendix B* and also clear from figure 1, the normalization condition $\int_{-\infty}^{\infty} \langle \rho_e \rangle de = N$ gives

$$e_0 \approx \frac{1}{3 b_0 \lambda} \sim 10^{-21} J \quad (39)$$

Following from eq.(35), the rapid decay of density of states for $e < 0$ implies very few levels in the edge region; this can directly be confirmed from eq.(33) which gives their number, say N_{edge} as

$$N_{edge}(e) = \int_{-\infty}^e \langle \rho_{edge-l}(e) \rangle de = \frac{N \mathcal{F}(\lambda b_0 e)}{\sqrt{\lambda^3}} = \frac{\mathcal{F}(\lambda b_0 e)}{\sqrt{\lambda_0^3}}. \quad (40)$$

with $\mathcal{F}(x) = \int_{-\infty}^x dx f_L(x)$. As can be seen from figure 2, \mathcal{F} is maximum at $e = 0$, with $\mathcal{F}(0) \approx 0.16$, and rapidly decays as $|e|$ increases. Clearly most of the contribution to f_0 is coming from the region $x \sim 0$, indicating the presence of almost all levels in the lower edge region very close to $e = 0$. Further the mean level spacing $\Delta(e)$ at an arbitrary energy e in the edge region is

$$\Delta(e) = \frac{1}{\langle \rho_{edge-l} \rangle} \approx \frac{\sqrt{\lambda}}{N b_0 f_L(\lambda b_0 e)}. \quad (41)$$

The above indicates $\Delta(0) \ll \Delta(e_l)$ with $e_l \ll 0$.

IV. HEAT CAPACITY OF THE BASIC BLOCK

Our next step is to calculate the ensemble averaged heat capacity C_v of a basic-block of volume Ω_b , defined as $\langle C_v \rangle = k \beta^2 \frac{\partial^2}{\partial \beta^2} \langle \log Z \rangle$ with Z as its partition function: $Z =$

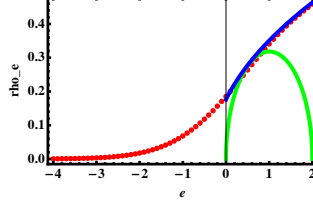


FIG. 1: **Finding e_0 where edge meets bulk?**: Bulk density of state $\rho_{bulk}(e)$ (eq.(31), green color) and the edge density of states $\rho_{edge}(e)$ (eq.(32) with $f(x)$ given by eq.(33), red dots). The approximation (37) of $\rho_{edge}(e)$ for $e > 0$ is also depicted by blue color.

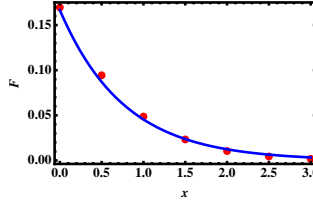


FIG. 2: **Counting function $\mathcal{F}(x) = \int_{-\infty}^x dx f_L(x)$ (see eq.(40))**: A rapid exponential decay of $\mathcal{F}(\lambda b_0 e)$ (red dots) away from $e = 0$ indicates most of the eigenvalues lie close to $e = 0$. The solid curve (blue color) describes the fit $(1/6)\exp[-1.3x]$

$\sum_{n=1}^N \exp[-\beta e_n]$. The latter can also be expressed as $Z = \int de \rho_e(e) \exp[-\beta e]$ with $\rho(e)$ as the density of states $\rho_e(e) = \sum_{n=1}^N \delta(e - e_n)$ of a typical basic block. For energy ranges where level-spacing is very small, $\rho(e)$ can be approximated by a smooth function i.e its spectral average. In the present case, however, the spectrum consists of regions with very large mean level spacing for $e < 0$ and it is appropriate to separate the discrete and continuous parts of Z [56]:

$$Z = \sum_{n; e_n < 0} \exp[-\beta e_n] + \int_0^{\infty} de \bar{\rho}_e \exp[-\beta e]. \quad (42)$$

with $\bar{\rho}_e$ as the spectral averaged density of states. Neglecting its fluctuations over basic block ensemble, one can approximate $\langle \log Z \rangle \approx \log \langle Z \rangle$. This in turn gives

$$\langle C_v \rangle = k \beta^2 \frac{\partial^2}{\partial \beta^2} \log \langle Z \rangle \quad (43)$$

where

$$\langle Z \rangle = \sum_{n; e_n < 0} \langle \exp[-\beta e_n] \rangle + \int de \langle \bar{\rho}_e \rangle \exp[-\beta e] \quad (44)$$

with $\langle \overline{\rho_e} \rangle$ as the level density averaged over the spectrum as well as the ensemble. (Note the first term here is not spectral averaged).

A. Calculation of $\langle Z \rangle$

Due to different functional behavior of the level density in the edge and bulk regions, we divide $\langle Z \rangle$ in four parts corresponding to lower edge ($-\infty < e \leq e_0$), bulk ($e_0 \leq e \leq (2/b) - e_0$) and upper edge ($(2/b) - e_0 < e \leq \infty$) respectively:

$$\langle Z \rangle = \sum_{n; e_n < 0} \langle \exp[-\beta e_n] \rangle + J_L + J_B + J_U \quad (45)$$

where

$$J_L = \int_0^{e_0} de \langle \rho_{edge-l}(e) \rangle \exp(-\beta e) \quad (46)$$

$$J_B = \int_{e_0}^{\frac{2}{b_0} - e_0} de \langle \rho_{bulk}(e) \rangle \exp(-\beta e) \quad (47)$$

$$J_U = \int_{\frac{2}{b_0} - e_0}^{\infty} de \langle \rho_{edge-u}(e) \rangle \exp(-\beta e) \quad (48)$$

Substituting eq.(32) in eq.(46), one can rewrite it as

$$J_L = \frac{N b_0}{\sqrt{\lambda}} \int_0^{e_0} de f_L(\lambda b_0 e) \exp(-\beta e) \quad (49)$$

In the region $0 < e < e_0$, f_L can be approximated by eq.(36). Substituting the latter in eq.(49) gives

$$J_L \approx \frac{N}{\pi} \left(\frac{1}{3\lambda\beta e_0} \right)^{3/2} \left[\gamma\left(\frac{3}{2}, (1+\eta)\beta e_0\right) - \gamma\left(\frac{3}{2}, \eta\beta e_0\right) \right] \exp[\eta\beta e_0] \quad (50)$$

where $\eta \approx 1$, $c_0^2 = (0.1865\pi)^2 \approx 1/3$ and $\gamma(a, x)$ is the incomplete Gamma function defined as $\gamma(a, x) = \int_0^x t^{a-1} e^{-t} dt$ with e_0 and λ given by eq.(38), eq.(39) respectively.

Similarly, J_B can be written as (with $\langle \rho_{bulk} \rangle$ given by eq.(31))

$$\begin{aligned} J_B &\approx \frac{N}{\pi} \int_{be_0}^{2-be_0} dx \sqrt{x(2-x)} e^{-\frac{\beta}{b}x} \quad (51) \\ &= \frac{N}{2\pi} \Phi\left(\frac{3}{2}, 3, -6\lambda\beta e_0\right) - \frac{N\sqrt{2}}{\pi} \left(\frac{1}{3\lambda\beta e_0}\right)^{3/2} \gamma\left(\frac{3}{2}, \beta e_0\right) - \frac{N\sqrt{6\lambda-1}}{9\pi\lambda^2\beta e_0} e^{-6\lambda\beta e_0} \quad (52) \end{aligned}$$

Due to presence of the term $e^{-\frac{\beta}{b}x}$ in the integrant, the contribution from the above integral is significant when $\beta e_0 < 1$ (i.e $k_B T > e_0$ or the temperature T is high enough to ensure the

thermal perturbation to access the states in the bulk). With $e_0 \approx (3b_0\lambda)^{-1}$, this requires $T > (3k_B b\lambda)^{-1} \sim 75^\circ K$. (with $\lambda \approx 495$, $b \sim 10^{18} J^{-1}$ and $k_b = 1.38 \times 10^{-23} J/K$).

Further J_U can be calculated by substituting eq.(32) with f_U given by eq.(34). As the integration-range now is $2 - be_0 < x < \infty$, the level-density decreases faster than exponential in this range and one can write

$$J_U \approx e^{-3\beta e_0} J_L. \quad (53)$$

This leaves the contribution from J_U significant only for large $3\beta e_0 < 1$ or $T > o(10^2) K$.

Substitution of eqs.(50,52, 53) in eq.(45) gives the partition function for the basic block

$$\begin{aligned} \langle Z \rangle = & \sum_{n; e_n < 0} \langle \exp[-\beta e_n] \rangle + \frac{N}{\pi} \left(\frac{1}{3\lambda\beta e_0} \right)^{3/2} \left[\gamma \left(\frac{3}{2}, (1 + \eta) \beta e_0 \right) - \gamma \left(\frac{3}{2}, \eta \beta e_0 \right) \right] e^{\eta\beta e_0} + . \\ & + \frac{N}{2\pi} \Phi \left(\frac{3}{2}, 3, -6\lambda\beta e_0 \right) - \frac{N\sqrt{2}}{\pi} \left(\frac{1}{3\lambda\beta e_0} \right)^{3/2} \gamma \left(\frac{3}{2}, \beta e_0 \right) - \frac{N\sqrt{6\lambda - 1}}{9\pi\lambda^2\beta e_0} e^{-6\lambda\beta e_0} \quad (54) \end{aligned}$$

A substitution of the above expression in eq.(43) gives, in principle, the specific heat. The above expression can further be simplified by noting that (i) only a single level is present in the tail region $e < 0$ and that too is very close to $e \sim 0$, one can approximate $\sum_{n; e_n < 0} \langle \exp[-\beta e_n] \rangle \approx 1$, (ii) for $x \gg 1$, $\Phi \left(\frac{3}{2}, 3, -x \right) \approx \frac{2}{\sqrt{\pi}} \frac{1}{\sqrt{x^3}}$ and $\gamma \left(\frac{3}{2}, x \right) \approx \Gamma \left(\frac{3}{2} \right) - (x)^{1/2} e^{-x}$. As, in the present work, our interest is in temperature regime $T < 100^\circ K$, this implies $\lambda\beta e_0 \gg 10^2$ (with e_0 given by eq.(39)) and one can then approximate

$$\langle Z \rangle \approx 1 + \frac{N}{\pi} \left(\frac{1}{3\lambda\beta e_0} \right)^{3/2} \left[\gamma \left(\frac{3}{2}, (1 + \eta) \beta e_0 \right) - \gamma \left(\frac{3}{2}, \eta \beta e_0 \right) \right] e^{\eta\beta e_0} \quad (55)$$

For comparison with the experiments however it is helpful to analyze the specific heat in different temperature regimes.

B. $\langle C_v \rangle$ for low temperatures T

Case (a): $\beta e_0 \gg 1$: As $k_b T \ll e_0$ here, the thermal perturbation mixes very few states even

in the lower edge. With $\beta e_0 \gg 1$ in this case, both γ -functions in eq.(55) can be expanded asymptotically as

$$\gamma(a, x) \approx \Gamma(a) - x^{a-1} e^{-x} \sum_{m=0}^{M-1} \frac{(-1)^m \Gamma(1 - a + m)}{\Gamma(1 - a) x^m} + O(x^M) \quad (56)$$

Following from the above, the 2nd and higher order terms in the series for $\gamma\left(\frac{3}{2}, (1+\eta)\beta e_0\right)$ are smaller than those of $\gamma\left(\frac{3}{2}, \eta\beta e_0\right)$ by an exponential factor and one can approximate $\gamma\left(\frac{3}{2}, (1+\eta)\beta e_0\right) \approx \Gamma(3/2)$. This along with eq.(60) reduces eq.(55) as

$$\langle Z \rangle \approx 1 + \frac{\sqrt{\eta^3}}{\pi \sqrt{27} \lambda_0^3} \sum_{m=0}^{M-1} \frac{(-1)^m \Gamma(m-1/2)}{\Gamma(-1/2) (\eta\beta e_0)^{m+1}} + O((\beta e_0)^M) \quad (57)$$

Substitution of eq.(61) in eq.(43) now leads to,

$$C_v(T) \approx \frac{k_b \sqrt{\eta^3}}{\pi \sqrt{27} \lambda_0^3} \sum_{m=0}^{M-1} \frac{(-1)^m (m+1)(m+2)\Gamma(m-1/2)}{\Gamma(-1/2) (\eta\beta e_0)^{m+1}} + O((\beta e_0)^M) \quad (58)$$

with $\eta \approx 1$, $\lambda_0 \approx \sqrt{2}$, $e_0 \sim 10^{-21} J$. At very low temperatures, the above indicates a linear T -dependence of the leading order term:

$$C_v(T) \approx 0.22 (\lambda b_0) k_b^2 T + 0.37 (\lambda b_0)^2 k_b^3 T^2 - 2.32 (\lambda b_0)^3 k_b^4 T^3 + O(T^4) \quad (59)$$

With increasing temperature, the approximation in eq.(61) is however not very good and the leading order term of $C_v(T)$ can behave as $T^{1+\varepsilon}$ with $0 < \varepsilon < 0.5$.

Case (b): $\beta e_0 \ll 1$

In limit $\beta e_0 \ll 1$, eq.(50) can be approximated by the behavior of $\gamma(a, x)$ near $x = 0$:

$$\gamma(a, x) = \sum_{n=0}^{\infty} (-1)^n \frac{x^{a+n}}{n! (a+n)}. \quad (60)$$

Substitution of the above in eq.(55) gives

$$\langle Z \rangle \approx 1 + \frac{\sqrt{2} e^{\eta\beta e_0}}{\pi \sqrt{27} \lambda_0^3} \sum_{m=0}^{M-1} a_m (\beta e_0)^m + O((\beta e_0)^M) \quad (61)$$

with $a_m = \frac{(-1)^m}{m!(m+3/2)} ((1+\eta)^{m+3/2} - \eta^{m+3/2})$. Substitution of the above in eq.(43) then leads to

$$C_v \approx \frac{k_b e^{\eta\beta e_0}}{\pi \sqrt{27} \lambda_0^3} \sum_{m=0}^{M-1} b_m (\beta e_0)^{m-2} + O((\beta e_0)^{(M+1)}) \quad (62)$$

with $b_m = \frac{(-1)^m}{m!} \left[\frac{\eta_0(m+2)}{(m+7/2)} - \frac{2\eta_0(m+1)}{(m+5/2)} + \frac{\eta_0(m)}{(m+3/2)} \right]$ and $\eta_0(m) = 2^{m+3/2} - 1$. The above gives the leading order term decaying as $\frac{1}{T^2}$.

C. Comparison with experiments

Specific heat experiments on a wide range of glasses indicate a super-linear dependence on temperature below $T \leq 1^{\circ}K$: $c_v \sim T^{1+\varepsilon}$, $\varepsilon \sim 0.1 \rightarrow 0.3$ and a bump in the plot c_v^{total}/T^3 vs T in the region near $T \sim 10^{\circ}K$. Although the available experimental results are in general applicable for glass solids of macroscopic size, it is tempting to compare them for those of microscopic size too. Previous studies have indicated that the thermal properties of solids at nano scales are in general different from macro scales. More specifically, the specific heat at nano scales is expected to be bigger than that of macro scales [28, 29, 32].

Theoretical results mentioned in previous section are derived for the heat capacity of a basic block of volume Ω_b . The specific heat corresponding to non-phononic contribution can then be given as

$$c_v = \frac{1}{\rho_m \Omega_b} \langle C_v \rangle. \quad (63)$$

with ρ_m as the mass-density of the glass. As discussed in [38], Ω_b can be expressed in terms of the molar mass M of the molecular units participating in dispersion interaction:

$$\Omega_b = \frac{64M}{\rho N_a} \quad (64)$$

with N_a as the Avogadro number. The total c_v of the block however consist of the contribution from phonons too:

$$c_v^{total} = c_v + c_v^{ph} \quad (65)$$

where

$$c_v^{ph} = \frac{9R}{M} \left(\frac{T}{T_D} \right)^3 \int_0^{T_D/T} dx \frac{x^4 e^x}{(e^x - 1)^2} \quad (66)$$

$$= \frac{R}{M x_D^3} \left[\frac{12\pi^4}{5} - 9(x_D^4 + 4x_D^3 + 12x_D^2 + 24x_D + 24)e^{-x_D} \right] \quad (67)$$

with $x_D = T/T_D$ and T_d as the Debye temperature and $R = 8.31$ as the gas constant. Contrary to bulk materials, T_D for nano materials can be affected by the size, composition and dimensionality. Experiments indicate T_D decreases with decreasing size [32].

The heat capacity formulation derived in previous section are expressed in terms of the mathematical functions and their correspondence with experimental results is not directly

obvious. For numerical analysis and comparison with experiments, it is instructive to directly substitute eq.(54) for the partition function and use computational techniques to obtain c_v^{total} .

Comparison below $T \sim 1^\circ \text{K}$: Figure 3 displays the comparison of theoretically predicted c_v^{total} for an amorphous SiO_2 basic block along with the experimental data for a macroscopic block taken from figure 6 of [26]. A good agreement is achieved if the Debye temperature T_D is taken much less than that for a macroscopic system. A lower The good agreement clearly indicates that the superlinearity of specific heat in glasses exist even at nano scales.

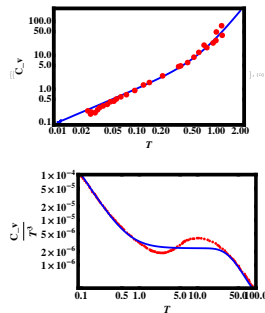


FIG. 3: Comparison of total specific heat (blocks+phonons) with experimental data: $c_v^{total} = c_v + c_v^{ph}$, with $c_v = \frac{1}{\rho_m \Omega_b} \langle C_v \rangle$ obtained from eqs.(54, 43) and c_v^{ph} from eq.(67) is displayed by the blue curve. Experimental data for Suprasil (red curve) is taken from figure 6 of [26] for *Top* case and from figure 1 of [26] for *bottom* case. The T_D value which seems to give a better fit in this case is much less than that of bulk; here $T_D = 190^\circ \text{K}$. Note $T_D \approx 495^\circ \text{K}$ for the macroscopic sizes of $a - SiO_2$ [2].

In connection with the specific heat below 1°K , there have been experimental reports indicating an absence of linear/ super-linear behavior in some types of bulk glass materials which has been attributed to absence of two level tunneling states [13–18]. Following discussion in previous section, we find that the linear temperature dependence regime of specific heat for the basic blocks depends on the competition between thermal perturbation and the density of states and is sensitive to the edge as well as bulk parameters λ, b ; for the cases in which $\lambda^2 b k_b \ll 1$ it may therefore move to ultra low temperatures.

Comparison above $T \sim 1^\circ \text{K}$: Figure 4 displays the total specific heat behavior

c_v^{total}/T^3 behaviour (obtained from eqs.(54, 43)) along with experimental result for $a - SiO_2$ taken from figure 1 of [26]; the theoretical results, although derived for a basic block, are almost consistent with experiments on macroscopic sizes of the glass. The bump in heat capacity for the latter, in the temperature regime near $T \sim 6^\circ \text{K}$, is however replaced by a plateau region. We believe that the small deviation beyond the bump can be corrected by an exact calculation of $\langle Z \rangle$ edge directly using eq.(32) instead of its approximate form; here $T_D = 190^\circ \text{K}$. Note $T_D \approx 495^\circ \text{K}$ for the macroscopic sizes of $a - SiO_2$ [2]).

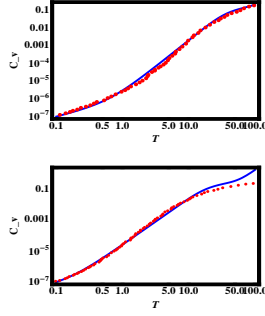


FIG. 4: Comparison of total specific heat with experimental data: $c_v^{total} = c_v + c_v^{ph}$, with c_v obtained from eqs.(54, 43) and c_v^{ph} from eq.(67), is displayed by the blue curve. *Top*: $a - SiO_2$ with $T_D = 200^\circ \text{K}$, *Bottom*: vitreous Se with $T_D = 113^\circ \text{K}$. Experimental data (red curve) for $a - SiO_2$ and vitreous Se is taken from figure and figure 12 of [1], respectively. The T_D value which seems to give a better fit in both cases is less than that of bulk. Note $T_D \approx 200^\circ \text{K}$ and 123°K for the macroscopic sizes of $a - SiO_2$ and $a - Se$ [2].

V. CONCLUSION

In the end, we summarize with our main ideas and results. We find that a range of dispersion forces acting between molecules introduce a natural length scale in an amorphous system leading to emergence of nano-scale sub-structures (referred as basic blocks in the texts). The complicated molecular interactions within one such block result in appearance of its Hamiltonian as a random matrix in the non-interacting product basis of single molecule states. Motivated by the physical reasoning discussed in ([38]), the size of the block is taken

to be the typical medium range order of glasses where Vanderwaal forces are known to dominate and lead to delocalization of the many-body states of the block Hamiltonian. The ensemble of block Hamiltonians can then be well-described by a Gaussian orthogonal ensemble (GOE), the standard random matrix model for systems with time-reversal symmetry. This is also confirmed by an explicit calculation of the ensemble averaged density of states of the block (based on the standard, averaged, Green's function approach) which turns out to be same as that of a GOE i.e a semi-circle in the bulk of the spectrum. The GOE density of states in the edge is known to undergo a super-exponential variation. Encouraged by the agreement in bulk, we assume GOE type behavior for the spectrum edge too; the specific heat for the block derived by the assumption agrees with experimental results.

Our analysis indicates that for temperatures below $T < 1^\circ K$ the specific heat C_v of the basic block depends on the competition between three energy scales, namely, thermal perturbation kT , the bulk spectrum parameter b and the edge spectral parameter λ . Based on whichever of these parameters dominates the partition function in eq.(45)), the specific heat of the basic block changes from a linear to super-linear temperature dependence. Using extensivity arguments, the results obtain in the present study can then be used to determine the specific heat of the macroscopic glass solid; this will be discussed elsewhere in detail.

An important point worth emphasizing is the absence of any adjustable parameters in our theory or their dependence on other microscopic universal ratios to explain the observable ones [19, 20, 22, 23, 37] (also see [24]). In fact, the two parameters b and λ , which appear in our specific heat formulation, depend only on the molecular properties e.g. polarizability, ionization energy, molecule volume and strengths of Vanderwaal interactions which are experimentally well-measured and a knowledge of their order of magnitudes is sufficient for our purpose. As discussed in the text, $b \sim 10^{18}$ and $\lambda \sim 3^{16/3}$ for a wide range of glasses which in turn predicts an analogous behavior of the low temperature specific heat for all these systems and is therefore in agreement with experimental observations.

Although the theoretical analysis presented here assumes the amorphous molecules to be non-polar and is therefore applicable in case of insulators, the information is used only in the order of magnitude calculation of the parameter b . The theory can therefore be extended to other types of amorphous systems too except now b has to be recalculated.

Acknowledgments

I am indebted to Professor Anthony Leggett for introducing me to this rich subject and continuous intellectual support in form of many helpful critical comments and insights over a duration of fourteen years in which this idea was pursued. I am also very grateful to Professor Michael Berry for advise in fundamental issues and important technical help in dealing with Airy function integrals which forms the basis of my calculation.

-
- [1] R.C. Zeller and R.O. Pohl, Phys. Rev. B, 4, 2029, (1971).
- [2] R. B. Stephens, Phys. Rev. B, 8, 2896, (1973).
- [3] R.O.Pohl, X.Liu and E.Thompson, Rev. Mod. Phys. 74, 991, (2002).
- [4] P.W. Anderson, B.I. Halperin and C.M. Verma, Philos. Mag. 25, 1, (1972).
- [5] W.A. Phillips, Two Level States in Glass, rep. Prog. Phys. 50, 1657, (1987); R. Hunklinger and K. Raychandharai, in Progr. Low-Temp. Phys. (ed. D. F. Brewer, Elsevier, Amsterdam), 9, 265, r1986; J. Jackle , *Amorphous Solids: Low-Temperature Properties*, (Springer, Berlin) 1981.
- [6] Y. M. Galperin, V. G. Karpov and N. Solovjev, Eksp. Teor. Fiz., 94 (1988) 373.
- [7] M.A. Ramos, Low Temp. Phys. 46, 104 (2020).
- [8] T. Prez-Castaeda, C. Rodriguez-Tinoco, J. Rodriguez-Viejo and M. A. Ramos, 111, 11275, (2014).
- [9] M. A. Ramos, T. Prez-Castaeda, R. J. Jimnez-Riobo, C. Rodriguez-Tinoco, and J. Rodriguez-Viejo, Low Temp. Phys. 41, 412 (2015);
- [10] A. J. Leggett and D. Vural, J. Phys. Chem. B, 42,117, (2013).
- [11] A.J. Leggett, Physica B: Cond. Matt. 169, 332 (1991).
- [12] C.C.Yu and A.J.Leggett, Comments Condens Matter Phys 14, 231, (1988).
- [13] T. Perez-Castaneda, C. Rodriguez-Tinoco, J. Rodriguez-Viejo and M. A. Ramos, PNAS, 111, 11275, (2014).
- [14] X. Liu et. al., Phys. Rev. Lett., 78, 4418, (1997).
- [15] B.L. Zink, R. Pietri and F. Hellman, Phys. Rev. Lett., 96, 055902, (2006).
- [16] D. R. Queen, X. Liu, J. Karel, T.H. Metcalf and F. Hellman, Phys. Rev. Lett., 110, 135901, (2013).
- [17] N.I. Agladze, A.J. Sivers, Phys. Rev. Lett., 80, 4209, (1998).
- [18] C. A. Angell, C.T. Moynihan and M. Hemmati, J. Non-Crystalline solids, 274, 319, (2000).
- [19] C.C.Yu, Phys. Rev. Lett., 63, 1160, (1989).
- [20] D. A. Parashin, Phys. Rev. B, 49, 9400, (1994).
- [21] D. Vural and A.J.Leggett, J. Non crystalline solids, 357, 19, 3528, (2011).
- [22] V. Lubchenko and P. G. Wolynes, Phys. Rev. Lett. 87, 195901, (2001).

TABLE I: **Specific heat calculation: relevant data for 18 glasses:** here the columns 3, 4 give the mass density ρ_m of the glass and the molar mass M of the relevant unit undergoing dispersion interaction (see [38] for details), respectively. This data is used in eq.(64) to obtain the volume of the basic block, displayed in column 5. The columns 6, 7, 8, 9 display the optical parameters for the glass, namely refractive index n_I , characteristic frequency ν_e , Hamaker constant A_H and edge-spectral parameter b (see eq.(20) and eq.(21,22) and *appendix c*); note A_H corresponds to non-retarded dispersion interaction (see eq.(11.14) of [43] or eq.(13b) of [53] with medium 2 as vacuum). From eq.(59), the specific heat for very low T can be expressed as $c_v = c_1 T + o(T^2)$; c_1 values for 18 glasses are given in column 10, along with available ones from [2].

Index	Glass	ρ_m	M	Ω_b	n_I	ν_e	A_H	b	c_1	$c_{1,stephen}$
Units		$\times 10^3 \frac{Kg}{m^3}$	$\frac{gm}{mole}$	10^4 angstroms^3		$\times 10^{15} \text{ sec}^{-1}$	$\times 10^{-20} J$	$\times 10^{18} J^{-1}$	$\frac{ergs}{gm-K^2}$	$\frac{ergs}{gm-K^2}$
1	a-SiO2	2.20	120.09	5.80	1.45	3.24	6.31	0.91	10	11
2	BK7	2.51	92.81	3.93	1.51	3.10	7.40	0.78	12	
3	As2S3	3.20	32.10	1.07	2.35	1.41	17.98	0.32	14	14
4	LASF	5.79	167.95	3.08	1.80	3.00	15.15	0.38	3	
5	SF4	4.78	136.17	3.03	1.72	1.98	8.40	0.68	7	
6	SF59	6.26	92.81	1.58	1.89	1.70	13.12	0.44	7	
7	V52	4.80	167.21	3.70	1.51	3.40	8.37	0.69	6	
8	BALNA	4.28	167.21	4.15	1.47	3.24	6.87	0.84	7	
9	LAT	5.25	205.21	4.15	1.51	3.79	9.16	0.63	4	
10	a-Se	4.30	78.96	1.95	1.90	2.56	13.34	0.43	8	7.5
11	Se75Ge25	4.35	77.38	1.89	3.64	0.68	24.88	0.23	4	
12	Se60Ge40	4.25	76.43	1.91	4.65	0.48	27.15	0.21	4	
13	LiCl:7H2O	1.20	131.32	11.63	1.39	3.19	4.75	1.21	13	
14	Zn-Glass	4.24	103.41	2.59	1.53	3.00	7.71	0.74	10	
15	PMMA	1.18	102.78	9.26	1.48	2.82	6.10	0.94	13	46
16	PS	1.05	27.00	2.73	1.56	2.15	6.03	0.95	49	51
17	PC	1.20	77.10	6.83	1.56	2.08	6.00	0.96	17	38
18	Epoxy	1.20	77.10	6.83	1.54	1.84	4.91	1.17	21	

- [23] M. Turlakov, Phys. Rev. Lett., 93, 035501, (2004).
- [24] A.L. Burin, J. Low. Temp. Phys. 100, 309 (1995); A.L.Burin and Y.Kagan, Physics Letters A, 215 (3-4), 191, (1996).
- [25] J. P. Sethna and K.S. Chow, Phase Tans. 5, 317 (1985); M. P. Solf and M.W.Klein, Phys. Rev. B 49, 12703 (1994).
- [26] J.C. Phillips, J. Non-crys. solids 43, 37, (1981); 34, 153, (1979).
- [27] S.R.Elliott, Nature, 354, 445, (1991).
- [28] L. Qiu, N. Zhu, Y. Feng, E. E. Michaelides, G. ya, D. Jing, X. Zhang, P. M. Norris, C. N. Markides, O. Mahian, Physics Reports 843, 1, (2020).
- [29] Y. D. Qu, X. L. Liang, X. Q. Kong, and W. J. Zhang, Physics of Metals and Metallography,(Pleiades Publishing Ltd.), 118, 528, (2017).
- [30] M. Hartmann, G. Mahler and O.Hess, arXiv:quant-ph/0312214v4.
- [31] G. Guisbiers and L. Buchaillot, Physics Letters A 374, 305, (2009).
- [32] Yan-Li Ma, Ke Zhu and Ming Li, Phys.Chem.Chem.Phys., 20, 27539, (2018); M. Singh, S. Lara and S. Tlali, Jou. Taibah University for Science 11 (2017) 922929; N. Arora, D. P. Joshi, U. Pachauri, Materials Today: Proceedings 4 (2017) 1045010454;
- [33] A.J.Stone, *The theory of intermolecular forces*, Oxford scholarship online, Oxford university Press, U.K. 2015.
- [34] H. Y. Kim, J. O. Sofod, D. Velegol, M. W. Cole, and A. A. Lucas, J. Chem. Phys. 124, 074504.190, (2006).
- [35] The NIM basis can be truncated for the following reason. The typical energy of excitation for electronic, vibrational and rotational level in molecules is of the order of 10^{-19} , 10^{-20} , 10^{-23} J respectively. The thermal perturbation at very low temperatures ($T < 30K$) is not strong enough to result in the electronic state excitations and the molecule remain in its electronic ground state. It could however cause transitions to its roto-vibrational excited states.
- [36] A. Uhlhert and S.R. Elliott, J. Phys.: Condens. Matter 6, L99, (1994).
- [37] M. Schechter and P.C.E. stamp, arXiv: 0910.1283, (2009); A. Gaita-Ario and M. Schechter, Phys. Rev. Lett. 107, 105504, (2011).
- [38] P. Shukla, to be submitted.
- [39] I.G.Kaplan and O.B. Rodimova, Sov. Phys. Usp. 21(11), 1978.
- [40] A.D.Buckingham, Adv. Chem. Phys. 12, 107, (1967).

- [41] For qualitative analysis, C_6 can be approximated by London's formula $C_6 \approx \frac{3}{2}\alpha^2 I$ with α as the molecular polarizability averaged over all orientations and I as the first ionization potential [33, 39, 42, 43]). (As mentioned in chapter 6 of [33], α is roughly proportional to molecular volume and ionization potentials do not differ much among different molecules). Similarly $C_9 \approx 3/4\alpha C_6$ (applying eq.(10.2.5) of [33] for identical molecules). Taking typical values of the molecular polarizability $\alpha \sim 10^{-30} \text{ m}^3$ and $I \sim 10^{-18} \text{ J}$, gives $C_6 \sim 10^{-78} \text{ J} - \text{m}^6$ and $C_9 \sim 10^{-108} \text{ J} - \text{m}^9$.
- [42] Although more exact expressions for C_6 and C_9 are also available e.g see chapter 4 of [33]) or eq.(2.34) to eq.(2.40) of [39] but London's formula gives fairly accurate values for interactions in a vacuum. These values are usually lower than more rigorously determined ones.
- [43] J. Israelachvili, Chapter 11, *Intermolecular and Surface Forces*, 3rd ed. Academic Press, (2011).
- [44] R.H. French, J. Am. Ceram. Soc., 83, 2117, (2000).
- [45] H-J Stockmann, **Quantum Chaos: an introduction**, Cambridge univ. Press (1999) (see page 79).
- [46] G. J. Rodgers and A. J. Bray, Phys. Rev. B, 37, 3557, (1998).
- [47] A. Khorunzhy and G. J. Rodgers, 38, 3300 (1997).
- [48] T. Guhr, G. A. Muller-Groeling and H. A. Weidenmuller, Phys. Rep. 299, 189 (1998).
- [49] M.L.Mehta, *Random Matrices*, Academic Press, (1991).
- [50] D. Turnbull and D. E. Polk, J. Non-crys. solids 8, 19, (1972).
- [51] C. Buchner, L. Lichenstein, H.-J. Freund, *noncontact atomic force microscopy, nanoscience technology*, S. Moira et. al. (eds.), Springer int. Pub. 2015, DOI. 10.11007/978 - 3 - 319 - 15588 - 3₁₆.
- [52] D.Ma, A.D.Stoica and X.-L. Wang, Nature Material 8, 30, (2009).
- [53] R.H.French, R.M.Cannon, L.K.DeNoyer and Y.-M. Chiang, Solid State Ionics, 75, 13, (1995);
- [54] L. Zhang, F. Gan and P. Wang, Applied Optics, 33, 50, (1994).
- [55] M.J. Weber, **Handbook of optical materials**, CRC Press (U.S.A), (2003).
- [56] In case of the standard formulation for the partition function, (with ground state assumed to be at $e = 0$), the lower and upper limits are $e = 0$ and ∞ , respectively. To avoid divergence of the integral at negative energies, extra care for the lower limit must be taken for the cases where the ground state occurs at $e < 0$. Following from eq.(33), although the theoretical form

of the density of states in our case extends to $e \rightarrow -\infty$, however as discussed in section III, very few i.e 1 – 2 levels exist in the region $e \sim 0$ even in large N limit (with N as size of the spectrum). Using a continuous form of the $\rho(e)$ is therefore not justified in this region and can introduce errors in the calculation.

[57] G.H. Abbady, K. A. Aly , Y. Saddeek and N. Afify, Bull. Mater. Sci., Indian Academy of Sciences, 1819, (2016); (DOI 10.1007/s12034-016-1328-239).

Appendix A: Derivation of eq.(27)

To obtain higher order traces, we expand $\text{Tr } \mathcal{H}^n$ in terms of the matrix elements,

$$\text{Tr } \mathcal{H}^n = \sum_{\mathcal{K}_1, \mathcal{K}_2, \dots, \mathcal{K}_n} \mathcal{H}_{\mathcal{K}_1 \mathcal{K}_2} \mathcal{H}_{\mathcal{K}_2 \mathcal{K}_3} \dots \mathcal{H}_{\mathcal{K}_{n-1} \mathcal{K}_n} \mathcal{H}_{\mathcal{K}_n \mathcal{K}_1} \quad (\text{A1})$$

As clear, the trace operation ensures that the terms always have a cyclic appearance. Let us first consider T_3 ; it can be written as $T_3 = \langle \text{Tr } \mathcal{H}^3 \rangle = \sum_{\mathcal{K}, J, L} \langle \mathcal{H}_{\mathcal{K}J} \mathcal{H}_{JL} \mathcal{H}_{L\mathcal{K}} \rangle$. Clearly it contains (i) the terms of type $\langle \mathcal{H}_{\mathcal{K}J} \mathcal{H}_{JL} \mathcal{H}_{L\mathcal{K}} \rangle$ for $\mathcal{K} \neq J \neq L$, (ii) the terms of type $\mathcal{L} = K \neq J$ or $\mathcal{L} = J \neq K$ or $\mathcal{K} = J \neq L$. (iii) the terms of type $\mathcal{L} = K = J$. As $\langle \mathcal{H}_{\mathcal{K}\mathcal{K}} \rangle = 0$ and different matrix elements are uncorrelated, a term can contribute only if all matrix elements appearing in it are paired. Thus the contribution from all three types of terms is zero and this gives

$$T_3 \approx \sum_{\mathcal{K}} \langle (\mathcal{H}_{\mathcal{K}\mathcal{K}})^3 \rangle \rightarrow 0 \quad (\text{A2})$$

where the last result follows due to rapid decay of higher-order moments of $\mathcal{H}_{\mathcal{K}\mathcal{K}}$ which can be seen from eq.(7).

Similarly T_4 can be written as

$$T_4 = \langle \text{Tr } \mathcal{H}^4 \rangle = \sum_{\mathcal{K}, J, L, M} \langle \mathcal{H}_{\mathcal{K}J} \mathcal{H}_{JL} \mathcal{H}_{LM} \mathcal{H}_{MK} \rangle \quad (\text{A3})$$

Again, due to zero mean of the matrix elements and a lack of correlations among them, the surviving terms in this case are the following: (i) $\sum_{\mathcal{K}, J, M} \langle \mathcal{H}_{\mathcal{K}J} \mathcal{H}_{JK} \mathcal{H}_{KM} \mathcal{H}_{MK} \rangle$, (ii) $\sum_{\mathcal{K}, J, L} \langle \mathcal{H}_{\mathcal{K}J} \mathcal{H}_{JL} \mathcal{H}_{LJ} \mathcal{H}_{JK} \rangle$, (iii) $\sum_{\mathcal{K}, J} \langle \mathcal{H}_{\mathcal{K}J}^4 \rangle$, (iv) $\sum_{\mathcal{K}} \langle \mathcal{H}_{\mathcal{K}\mathcal{K}}^4 \rangle$. To proceed further, we note that the sum containing the same matrix element repeatedly are of the lower order in g_0 than the sums with pairs. This can be explained as follows: the terms of type (i, ii, iii) contain contributions from n -plet, $n = 1 \rightarrow g_0$, with lower-plets dominating the

higher-plets in strength but latter being more in number their total contribution may not be negligible. Considering only the 2-plets, their numbers in the sums of types (i, ii, iii) are $O(Ng_0^4), O(Ng_0^4), O(Ng_0^2)$. Clearly the sum of type (i, ii) dominate over (iii) even if one considers the contribution from 2-plets and ignores the higher ones. Proceeding similarly it can be seen that the higher order plets contributing to sum in type (i, ii) are much larger in number relative to sum in type (iii). Further the the sum in type (iv) is much smaller than (i,ii, iii); this follows because the number of terms in type (iv) are $O(N)$ and an off-diagonal matrix element forming a lower-plet is stronger than a typical diagonal. In large N -limit, therefore T_4 is dominated by the terms with pairwise-correlations and can be approximated as

$$T_4 \approx \sum_{\mathcal{K},J} v_{\mathcal{K}J} \langle (\mathcal{H}^2)_{\mathcal{K}\mathcal{K}} \rangle + \sum_{\mathcal{K},J} v_{\mathcal{K}J} \langle (\mathcal{H}^2)_{\mathcal{J}\mathcal{J}} \rangle \quad (\text{A4})$$

But as

$$\langle (\mathcal{H}^2)_{\mathcal{K}\mathcal{L}} \rangle = \sum_{\mathcal{M}} \langle \mathcal{H}_{\mathcal{K}\mathcal{M}} \mathcal{H}_{\mathcal{L}\mathcal{M}} \rangle = \delta_{\mathcal{K}\mathcal{L}} \sum_{\mathcal{M}} v_{\mathcal{K}\mathcal{M}}, \quad (\text{A5})$$

eq.(A4) can be rewritten as

$$T_4 \approx \sum_{\mathcal{K},J,L} v_{\mathcal{K}J} v_{\mathcal{K}L} + \sum_{\mathcal{K},J,L} v_{\mathcal{K}J} v_{\mathcal{J}L} = 2 \sum_{\mathcal{K}} \left(\sum_{\mathcal{J}} v_{\mathcal{K}J} \right)^2 = \frac{N}{2b^4} \quad (\text{A6})$$

where the last step follows from eq.(20). Similarly,we have

$$\begin{aligned} T_6 &\approx 2 \sum_{\mathcal{K},J} v_{\mathcal{K}J} \langle (\mathcal{H}^4)_{\mathcal{K}\mathcal{K}} \rangle + \sum_{\mathcal{K},J} v_{\mathcal{K}J} \langle (\mathcal{H}^2)_{\mathcal{J}\mathcal{J}} \rangle \langle (\mathcal{H}^2)_{\mathcal{K}\mathcal{K}} \rangle \\ &= 4 \sum_{\mathcal{K},J,L} v_{\mathcal{K}J} \langle (\mathcal{H}^2)_{\mathcal{K}\mathcal{L}} \rangle \langle (\mathcal{H}^2)_{\mathcal{L}\mathcal{K}} \rangle + \sum_{\mathcal{K},J,L,M} v_{\mathcal{K}J} v_{\mathcal{J}L} v_{\mathcal{K}M} \end{aligned} \quad (\text{A7})$$

Further using eq.(A5), we get

$$T_6 = 5 \sum_{\mathcal{K},J,M,S} v_{\mathcal{K}J} v_{\mathcal{K}M} v_{\mathcal{K}S} = 5 \sum_{\mathcal{K}} \left(\sum_{\mathcal{J}} v_{\mathcal{K}J} \right)^3 = \frac{5N}{8b^6} \quad (\text{A8})$$

We now proceed to calculate T_{2n} directly:

$$T_{2n} = \sum_{\mathcal{K}} \langle (\mathcal{H}^{2n})_{\mathcal{K}\mathcal{K}} \rangle = \sum_{\mathcal{K},L} \langle \mathcal{H}_{\mathcal{K}\mathcal{L}} (\mathcal{H}^{2n-1})_{\mathcal{L}\mathcal{K}} \rangle \quad (\text{A9})$$

For a given term to survive the averaging, one of the factors of \mathcal{H}^{2n-1} must be identical with $\mathcal{H}_{\mathcal{L}\mathcal{K}}$. As each one of the $(2n - 1)$ factors can play that

role, we have $T_{2n} = \sum_{s=0}^{n-1} \sum_{\mathcal{K},J} \langle \mathcal{H}_{\mathcal{K}J} (\mathcal{H}^{2s})_{\mathcal{J}J} \mathcal{H}_{\mathcal{J}K} (\mathcal{H}^{2n-2s-2})_{\mathcal{K}K} \rangle = \sum_{s=0}^{n-1} \sum_{\mathcal{K},J} \langle \mathcal{H}_{\mathcal{K}J}^2 \rangle \langle (\mathcal{H}^{2s})_{\mathcal{J}J} \rangle \langle (\mathcal{H}^{2(n-s-1)})_{\mathcal{K}K} \rangle$ which can be rewritten as

$$T_{2n} = \sum_{s=0}^{n-1} \sum_{\mathcal{K},J} v_{\mathcal{K}J} \langle (\mathcal{H}^{2s})_{\mathcal{J}J} \rangle \langle (\mathcal{H}^{2(n-s-1)})_{\mathcal{K}K} \rangle \quad (\text{A10})$$

Proceeding similarly as for T_4 and T_6 , one can show that $T_{2n} \approx \frac{1}{n+1} \binom{2n}{n} \frac{N}{2^n b^{2n}}$. Further, as in the case of T_3 , all odd ordered traces contain at least one unpaired term which leads to $T_{2n+1} \rightarrow 0$.

Appendix B: Finding e_0 where edge meets bulk

With bulk and the edge level densities given by eq.(31) and eq.(32) respectively, the form of the edge level density is different from that of bulk and it is important to know how and where they connect. Let the edge meet the bulk near $e = e_0$ with e_0 very small, but positive energy. The latter is needed to ensure a gapless spectrum because the bulk density is zero at $e = 0$ but edge-density is not. As mentioned in section III, the point e_0 where edge behavior smoothly joins the bulk behavior can be given by the requirement that

$$\langle \rho_{edge-l}(e_0) \rangle = \langle \rho_{bulk}(e_0) \rangle \quad (\text{B1})$$

Using the large x behavior of Airy functions i.e $Ai(-x) \sim \frac{1}{\pi^{1/2} x^{1/4}} \cos\left(\frac{2}{3} x^{3/2} - \frac{\pi}{4}\right)$, $Ai'(-x) \sim \frac{x^{1/4}}{\pi^{1/2}} \sin\left(\frac{2}{3} x^{3/2} - \frac{\pi}{4}\right)$, $\int Ai(-x) dx \sim \frac{1}{2\pi^{1/2} x^{3/4}} \cos\left(\frac{2}{3} x^{3/2} + \frac{\pi}{4}\right)$, it is easy to show that

$$f(x) \approx \frac{1}{\pi} \sqrt{c_0^2 + x} + \frac{1}{\pi x} \cos\left(\frac{2}{3} x^{3/2}\right). \quad (\text{B2})$$

The above gives $\langle \rho_{edge-l}(e) \rangle \approx \frac{\xi b_0}{\pi} \sqrt{c_0^2 + \lambda b_0 e}$ for $e > 0$. Our next step is to figure out what is ξ and λ ? For this we note that the functional form of both $\rho_{bulk}(e)$ and $\rho_{edge-l}(e)$ should match near $e \sim e_0$.

Substitution of the latter along with eq.(31) in eq.(B1) gives

$$\xi \sqrt{c_0^2 + \lambda b_0 e_0} = \sqrt{2b_0 e_0} \quad (\text{B3})$$

Using $\xi \sqrt{\lambda} = 1$ and $c_0^2 = 1/3$ in the above, we have

$$e_0 = \frac{c_0^2}{b_0 \lambda} \approx \frac{1}{3b_0 \lambda} \quad (\text{B4})$$

To find out exactly the point e_0 i.e where $f(x)$ in eq.(33) begins to behave as a square-root, we take help of Mathematica which gives $\lambda b e_0 \approx 3$ and therefore (See also figure 1)

$$e_0 \approx \frac{1}{3\lambda b_0}. \quad (\text{B5})$$

Appendix C: Calculation of J_B

Using eq.(31), the integral J_B can be written as

$$J_B = \frac{1}{\pi} \int_{b_0 e_0}^{2-b_0 e_0} dx \sqrt{x(2-x)} e^{-\frac{\beta}{b_0} x} \quad (\text{C1})$$

where $e_0 \approx \frac{3}{\lambda b_0}$ (as given by eq.(39)). As an exact evaluation of the above integral in terms of known functions is not available, we need to consider approximations. The exponential is the dominating term in the above integral and therefore dictates the approximation. By rearranging the integral limits, eq.(C1) can be rewritten as

$$J_B = \frac{1}{2\pi} \Phi\left(\frac{3}{2}, 3, -\frac{2\beta}{b_0}\right) - \frac{1}{\pi} I_B \quad (\text{C2})$$

where $\Phi(a, b; x)$ is a confluent Hypergeometric function, defined as $\Phi(a, b_0; x) = \int_0^2 dx \sqrt{x(2-x)} e^{-\frac{\beta}{b_0} x}$ and $I_B = \int_0^{b_0 e_0} dx \sqrt{x(2-x)} \left(e^{-\frac{\beta x}{b_0}} - e^{-\frac{\beta}{b_0}(2-x)} \right)$. Noting that the upper integration limit is $b_0 e_0 \sim 3/\lambda$ with $\lambda \gg 1$, one can approximate $2 - b_0 e_0 \approx 2$ which leads to

$$I_B \approx \sqrt{2} \left(\frac{b}{\beta}\right)^{3/2} \gamma\left(\frac{3}{2}, \beta e_0\right) - \frac{\sqrt{6\lambda - 1}}{9\pi\lambda^2\beta e_0} e^{-6\lambda\beta e_0} \quad (\text{C3})$$

Appendix D: Refractive indices of 18 Glasses

:

As mentioned near eq.(21), the zero frequency refractive index n_0 and characteristic frequency ν for low index material can be determined from the following equation

$$n(\nu)^2 - 1 = \mathcal{G}_{UV} + \frac{\nu^2}{\nu_e^2} (n(\nu)^2 - 1) \quad (\text{D1})$$

For cases where the refractive index for many wavelengths are available, least square fit to plot $(n^2 - 1)$ vs $(n^2 - 1)/\lambda^2$ can be used to extract the slope and intercept. The available

data for $n(\lambda)$ however varies from one glass to another. For example, in case of flouride glasses, $n(\lambda)$ vs λ dependence can be obtained from following relation from [54]

$$n(\lambda)^2 = 1 + \sum_{k=1}^6 \frac{f_k \lambda^2}{(\lambda^2 - \lambda_k^2)} \quad (\text{D2})$$

with λ_k as the wavelengths in ultraviolet (for $k = 1, 2, 3$) and infra-red regime (for $k = 4, 5, 6$), with f_k as the corresponding oscillator strengths; their values are obtained following the steps given in [54]) and displayed in table IV. For other glasses however $n(\lambda)$ is available only for few wavelengths and is given in tables V, VI.

In case of *Zn – glass*, we could find the refractive index of one of its components, namely $NaPo_3$ only for one wavelength; the refractive index for glass was then obtained by using the standard relation for glass-ceramics i.e $n = \sum_k w_k n_k \rho M_k / \rho_k M$, with w_k as the weight fraction of the component, ρ_k as the mass density, M_k as the molar volume, n_k as its refractive index in the glass; using $(n, w, \rho, M) = (1.547, 0.6, 4.95, 129.2280)$, $(1.4746, 0.2, 4.893, 175.3238)$ and $1.4037, 0.2, 2.181, 101.9617$ for $ZnF_2, BaF_2, NaPo_3$ respectively, with refractive indices for components given at $\lambda = 5876$ AA [55]. Substitution of these values in the above formula then gives $n = 1.5281$ for Zn-Glass; its A_H was then obtained from eq.(21) (due to lack of information for its characteristic frequency).

TABLE II: Data for eq.(D2) for Floride-glassess (all wavelength are in μm) [54]

Glass	λ_1, f_1	λ_2, f_2	λ_3, f_3	λ_4, f_4	λ_5, f_5	λ_6, f_6
Lat	0.0735, 1.2429	0.1050, 1.3855	0.0828, 1.3044	17.5479, 1.4821	44.4379, 2.7631	25.2953, 1.7069
BALNA	0.07345, 0.6746	0, 0	0.1105, 0.494	17.4112, 0.8214	0, 0	42.6812, 1.7876
LAT	0.0735, 0.7457	0.084, 0.5341	0, 0	17.5479, 0.8893	26.1515, 0.8034	0, 0

TABLE III: Refractive indices of glasses [55]: here columns 2 – 7 give the refractive indices, of the glasses listed in 1st column, for the given wavelength (in μm), with $\lambda_1 = 0.6328$, $\lambda_2 = 0.5893$, $\lambda_3 = 0.5876$, $\lambda_4 = 0.5461$, $\lambda_5 = 0.4800$, $\lambda_6 = 0.4358$

Glass	λ_1	λ_2	λ_3	λ_4	λ_5	λ_6
a-SiO2			1.4585			1.4667
BK7	1.5151	1.5168		1.5187	1.5228	1.5267
As2S3	2.465	2.48	2.521	2.5620	2.636	
LASF7		1.850				
SF4		1.7551	1.7912			
SF59	1.9432	1.962	1.9635	1.9890	2.0156	
a-Se			2.4153			2.45
Se75Ge25			2.9733			2.6554
Se60Ge40			3.2734			2.79
LiCl:7H2O			1.3939			1.4013
Zn-Glass			1.5281			
ET1000			1.4585			1.4667
:						

TABLE IV: Refractive indices of Polymers [55]: here each column gives the refractive indices of the listed polymers for the given wavelength (in μm), with $\lambda_1 = 1.0520$, $\lambda_2 = 0.8790$, $\lambda_3 = 0.8330$, $\lambda_4 = 0.7030$, $\lambda_5 = 0.6328$, $\lambda_6 = 0.5893$, $\lambda_7 = 0.5876$, $\lambda_8 = 0.4861$, $\lambda_9 = 0.4368$

Glass	λ_1	λ_2	λ_3	λ_4	λ_5	λ_6	λ_7	λ_8	λ_9
PMMA	1.481	1.483	1.484	1.486	1.489	1.491	1.491	1.497	1.502
PS	1.576	1.576	1.577	1.575	1.587	1.589	1.592	1.606	1.617
PC	1568	1.568	1.569	1.582	1.580	1.586	1.585	1.599	1.612